RESEARCH ARTICLE

AMERICAN JOURNAL OF medical genetics PART A

Microarray and FISH-Based Genotype–Phenotype Analysis of 22 Japanese Patients With Wolf–Hirschhorn Syndrome

Kenji Shimizu,[1,2] Keiko Wakui,[1] Tomoki Kosho,[1]* Nobuhiko Okamoto,[3] Seiji Mizuno,[4] Kazuya Itomi,[5] Shigeto Hattori,[6] Kimio Nishio,[7] Osamu Samura,[8] Yoshiyuki Kobayashi,[9] Yuko Kako,[10] Takashi Arai,[11] Tsutomu Oh-ishi,[11] Hiroshi Kawame,[12] Yoko Narumi,[1] Hirofumi Ohashi,[2] and Yoshimitsu Fukushima[1]

[1]Department of Medical Genetics, Shinshu University School of Medicine, Matsumoto, Japan

[2]Division of Medical Genetics, Saitama Children's Medical Center, Saitama, Japan

[3]Department of Medical Genetics, Osaka Medical Center and Research Institute for Maternal and Child Health, Osaka, Japan

[4]Department of Pediatrics, Central Hospital, Aichi Human Service Center, Kasugai, Aichi, Japan

[5]Department of Pediatric Neurology, Aichi Children's Health and Medical Center, Obu, Aichi, Japan

[6]Department of Pediatrics, Gunma University Hospital, Maebashi, Japan

[7]Department of Neonatology, Seirei-Hamamatsu General Hospital, Hamamatsu, Shizuoka, Japan

[8]Department of Obstetrics and Gynecology, NHO Kure Medical Center and Chugoku Cancer Center, Kure, Japan

[9]Department of Pediatrics, Hiroshima University Hospital, Hiroshima, Japan

[10]Department of Pediatrics, Showa University School of Medicine, Tokyo, Japan

[11]Division of Clinical Laboratory, Saitama Children's Medical Center, Saitama, Japan

[12]Department of Genetic Counseling, Graduate School of Humanities and Science, Ochanomizu University, Tokyo, Japan

Manuscript Received: 27 April 2013; Manuscript Accepted: 30 September 2013

Wolf–Hirschhorn syndrome (WHS) is a contiguous gene deletion syndrome of the distal 4p chromosome, characterized by craniofacial features, growth impairment, intellectual disability, and seizures. Although genotype–phenotype correlation studies have previously been published, several important issues remain to be elucidated including seizure severity. We present detailed clinical and molecular-cytogenetic findings from a microarray and fluorescence in situ hybridization (FISH)-based genotype–phenotype analysis of 22 Japanese WHS patients, the first large non-Western series. 4p deletions were terminal in 20 patients and interstitial in two, with deletion sizes ranging from 2.06 to 29.42 Mb. The new Wolf–Hirschhorn syndrome critical region (WHSCR2) was deleted in all cases, and duplication of other chromosomal regions occurred in four. Complex mosaicism was identified in two cases: two different 4p terminal deletions; a simple 4p terminal deletion and an unbalanced translocation with the same 4p breakpoint. Seizures began in infancy in 33% (2/6) of cases with small (<6 Mb) deletions and in 86% (12/14) of cases with larger deletions (>6 Mb). Status epilepticus occurred in 17% (1/6) with small deletions and in 87% (13/15) with larger deletions. Renal hypoplasia or dysplasia and structural ocular anomalies were more prevalent in those with larger deletions. A new susceptible region for seizure occurrence is suggested between 0.76 and 1.3 Mb from 4pter,

How to Cite this Article:
Shimizu K, Wakui K, Kosho T, Okamoto N, Mizuno S, Itomi K, Hattori S, Nishio K, Samura O, Kobayashi Y, Kako Y, Arai T, Oishi T, Kawame H, Narumi Y, Ohashi H, Fukushima Y. 2014. Microarray and FISH-based genotype–phenotype analysis of 22 Japanese patients with Wolf–Hirschhorn syndrome.
Am J Med Genet Part A 164A:597–609.

Conflict of interest: none.
Grant sponsor: Japanese Ministry of Health, Labour and Welfare.
*Correspondence to:
Tomoki Kosho, M.D., Department of Medical Genetics, Shinshu University School of Medicine, 3-1-1 Asahi, Matsumoto 390-8621, Japan.
E-mail: ktomoki@shinshu-u.ac.jp
Article first published online in Wiley Online Library (wileyonlinelibrary.com): 19 December 2013
DOI 10.1002/ajmg.a.36308

encompassing *CTBP1* and *CPLX1*, and distal to the previously-supposed candidate gene *LETM1*. The usefulness of bromide therapy for seizures and additional clinical features including hypercholesterolemia are also described.

Key words: Wolf–Hirschhorn syndrome; 4p deletion; microarray analysis; fluorescence in situ hybridization (FISH); mosaicism; genotype–phenotype correlation; seizures

INTRODUCTION

Wolf–Hirschhorn syndrome (WHS, OMIM#194190), first described independently by Hirschhorn et al. [1965] and Wolf et al. [1965], is a contiguous gene deletion syndrome of the distal 4p chromosome characterized by a distinctive facial appearance, pre- and postnatal growth impairment, intellectual disability, and seizures [Battaglia et al., 2008]. In recent years, chromosomal microarray-based analysis has enabled us to identify WHS patients harboring well-defined variable-sized 4p deletions with or without additional duplications of other chromosomal regions as a result of unbalanced derivatives determined by concurrent metaphase fluorescence in situ hybridization (FISH) analysis [South et al., 2008c; Zollino et al., 2008].

Detailed genotype–phenotype correlation studies have also been performed using FISH analysis [Battaglia et al., 1999; Zollino et al., 2000] and chromosomal microarray analysis [Battaglia et al., 2008; Maas et al., 2008; South et al., 2008c; Zollino et al., 2008]. Clinical severity generally correlates with deletion sizes, although co-existing duplicated chromosomal regions, sequence variation of the gene(s) in the non-deleted 4p region, and other genetic backgrounds can all contribute to phenotypic variation [South et al., 2008c; Zollino et al., 2008]. Seizures represent a major clinical challenge in patients with WHS [Battaglia et al., 2009]. A review by Zollino et al. [2008] showed a high prevalence of seizures in patients with WHS regardless of the deletion sizes: 96% in those with <3.5 Mb deletions, 80% in those with 5–18 Mb deletions, and 90% in those with >22 Mb deletions. However, it remains unclear whether the severity of seizures in WHS patients might correlate with deletion sizes.

A WHS critical region, responsible for cardinal WHS features such as distinctive faces, growth/developmental delay, and seizures, was initially mapped to a 165-kb interval (WHSCR1) involving the entire *WHSC2* gene and the proximal part of *WHSC1* [Wright et al., 1997]. Additional reports of WHS patients with deleted regions distal to WHSCR1 suggested a new critical region (WHSCR2) involving the distal part of *WHSC1* and the entire *LETM1* gene, and these two genes have been considered the molecular hallmark of WHS [Zollino et al., 2003; Rodriguez et al., 2005]. Indeed, *WHSC1* is hypothesized as the gene that contributes to the main WHS phenotype of developmental delay and characteristic facial features [Nimura et al., 2009; Izumi et al., 2010]. *LETM1*, encoding a mitochondrial Ca^{2+}/H^{+} antiporter [Jiang et al., 2009], is thought to be the major candidate gene for seizures in patients with WHS [Rauch et al., 2001; South et al., 2007], while *FGFRL1*, located distal to WHSCR1/WHSCR2 and involved in bone cartilage formation during embryonic development, might be another candidate gene for craniofacial features of WHS [Catela et al., 2009; Engbers et al., 2009]. Other genes localized around these critical regions might also contribute to the various features of WHS.

Here, we present detailed clinical, microarray, and FISH-based molecular-cytogenetic findings of 22 Japanese patients with WHS, representing the first large series in a non-Western country.

MATERIALS AND METHODS

Patients

Twenty-two WHS patients from eight hospitals were included in this study between January 2010 and February 2012. The diagnosis of WHS was made from clinical characteristics as well as G-banded karyotyping with or without FISH analysis using a WHSCR or 4p subtelomeric probe. Written informed consent was obtained from all parents of the patients. Clinical information was collected by the clinical geneticists of each hospital and reviewed by one of them (K.S.). Ethical approval for this study was granted by the Institutional Review Board of Shinshu University School of Medicine, Matsumoto, Japan.

Chromosomal Microarray Analysis

Genomic DNA was isolated using standard protocols from the peripheral blood leukocytes of each patient. Chromosomal microarray analysis was performed through two whole genome oligonucleotide-based array platforms. NimbleGen CGX Array™ (Roche NimbleGen, Inc., Madison, WI) was used in the analyses of 21 patients, and includes 134,829 probes with an average resolution of 35 kb throughout the genome and 10 kb in clinically significant regions. Procedures for DNA labeling and microarray analysis were performed according to the manufacturer's instructions. The fluorescence signals on array slides were analyzed using a NimbleScan™ (Roche NimbleGen, Inc.), and presentation of array results was obtained by Genoglyphix® Software (Signature Genomics Laboratories, Spokane, WA). The Agilent Human Genome Microarray Kit 244A™ (Agilent Technologies, Santa Clara, CA) was used in the analysis of one patient, and includes 243,504 probes with a median probe space of 7.4 and 13.4 kb in intragenic and intergenic genomic sequences, respectively. Labeling and hybridization were performed according to the manufacturer's instructions, followed by scanning with an Agilent Microarray Scanner™ and data extraction with Feature Extraction Software™ (v9.5.3). The results were analyzed using Cytogenomics 2.0 Software™ (Agilent Technologies). Genomic coordinates of both array results were indicated according to NCBI build 36 (hg 18).

Metaphase FISH Analysis

To confirm cytogenetic rearrangements resulting in 4p deletion, FISH analysis using Bacterial Artificial Chromosome (BAC) probes was performed on metaphase chromosomes from peripheral blood leukocytes of all patients. We selected BAC probes around deleted regions of 4p and around other terminal duplicated segments in patients who were predicted to have unbalanced rearrangements

according to microarray results. Parental blood samples, where available, were also assayed with metaphase FISH to define whether chromosomal derivatives were de novo or inherited from parental balanced rearrangements. When a mosaic chromosomal abnormality was detected by G-banded karyotyping or suspected by chromosomal microarray results that showed a lower absolute $\log_2$ ratio than observed in patients with complete deletions or duplications, FISH analysis was performed on over 30 cells to detect a mosaic ratio.

RESULTS

Molecular-Cytogenetic Findings

Molecular-cytogenetic findings are summarized in Table I. G-banded chromosome analysis at the 400–550 band level, which was performed prior to this study, was abnormal in 18/22 (82%) patients: with terminal deletions of 4p in eight patients, interstitial deletions in three, additional materials of unknown origin attached to 4p in six, and mosaic chromosomes for a del(4)(p15.3p16.1) cell line (interstitial deletion) and a normal 46,XX cell line in Patient 15. G-banded chromosomes were normal in other patients who were found to have a deletion of 4p by FISH analysis using a 4p subtelomeric probe.

Chromosomal microarray analysis revealed 4p deletions to be terminal in 20 patients and interstitial in the other 2 patients. Deletion sizes ranged from 2.06 to 29.42 Mb, and all included WHSCR2 (Fig. 1). In patients with 4p terminal deletions, those $\leq$5.26 Mb were not detected by G-banded karyotyping. Only three patients (Patients 10, 11, and 12) shared the same breakpoints between 8.77 Mb (minimum) and 9.41 Mb (maximum) from the 4p terminus, corresponding to the loci of olfactory receptor (OR) gene clusters. Duplicated chromosomal regions accompanied by 4p deletion included 772 kb of terminal 10q in Patient 1, 45.6 Mb of terminal 4q in Patient 3, 6.9 Mb of terminal 8p in Patient 11, and 1.27 Mb of terminal 11q in Patient 20. In Patient 20, $\log_2$ values for probes spanning the duplicated 11q region were approximately 0.365 (theoretical $\log_2$ value of non-mosaic duplication, 0.58), which suggested that the duplication was mosaic (Fig. 2A).

FISH analysis using BAC probes designed according to microarray results confirmed a derivative chromosome 4 consisting of a duplicated 4q segment on the deleted 4p in Patient 3, and unbalanced translocations between 4p and 10q in Patient 1, and between 4p and 8p in Patient 11. In Patient 20, metaphases with an unbalanced translocation, der(4)t(4;11)(p15.31;q25), were found in 22/30 cells; and those with a simple terminal deletion, del(4)(p15.31), were found in 8/30 cells. The breakpoint of 4p was considered to be identical in both cell lines (21.0 Mb from 4pter; Fig. 2B, C). In Patient 15, metaphases with del(4)(p15.33) (11.9–12.1 Mb deletion) were found in 45/56 cells and those with del(4)(p16.3) (2.48–2.66 Mb deletion) were found in 11/56 cells (Fig. 3B, C), although only the larger deletion was demonstrated in microarray analysis (Fig. 3A). In nine patients whose parental samples were available, eight were found to have de novo deletions and the other (Patient 11) was found to have a maternal unbalanced translocation.

Clinical Findings and Correlation With Genotype

Clinical findings are summarized in Table II and major structural defects are listed according to deletion size in Table III. We categorized patients according to their deletion sizes into "small" with 4p terminal deletions less than 6 Mb (Patients 1–6), "intermediate" with deletions ranging from 6 to 15 Mb (Patients 7–17), and "large" with deletions over 15 Mb (Patients 18–22).

Neurological Features

Seizures began in 20/21 (95%) patients within the first three years of life (1 month to 2 years and 6 months old). Patient 10 was excluded because he was only 7 months old at the time of this study and might be expected to develop seizures in the future. Only Patient 13, aged 12 years with an 8.8 Mb interstitial deletion, had no seizures. The onset of seizures was late, occurring over 1 year of age, in 4/6 (67%) patients with small deletions (<6 Mb); and it was early, under 1 year of age, in 12/14 (86%) patients with larger deletions (>6 Mb). Status epilepticus occurred in 14/20 (70%) patients: 1/6 (17%) in those with small deletions and 13/14 (93%) in those with larger deletions. Seizures were intractable in six patients of ages ranging from 9 months to 6 years (median, 3 years and 7 months old), while seizures improved or disappeared in 14 patients of ages ranging from 1 year and 8 months to 18 years (median, 6 years and 2 months old). Potassium or sodium bromide was administered to four patients and the daily dose of bromide was 450 mg in Patient 7, 560 mg in Patient 8, 200 mg in patient 14, and 400 mg in Patient 18 at the time of this study. Seizures decreased in all of these. Patient 7 and Patient 8 showed a particularly obvious improvement after bromide therapy started at the ages of 1 year and 3 years, respectively. Neuroimaging demonstrated structural central nervous system defects in 9/18 (50%) patients, including periventricular leukomalacia, ventricular enlargement, hypoplasia of the corpus callosum, and cerebral or cerebellar atrophy.

A total of 19/22 (86%) patients showed severe developmental delay, while the other 3 patients showed a moderate delay. Independent walking was achieved in seven patients, including one with no seizures and five with no history of status epileptics.

Other Clinical Findings

Typical craniofacial features were present in all the patients except for Patient 1 with the smallest sized deletion (2.06 Mb; Fig. 4A) and Patient 13 with an interstitial deletion (1.37–10.22 Mb; Fig. 4H), both showing subtle features without the Greek warrior helmet appearance. The severity of short stature varied among patients regardless of the deletion sizes and the deleted regions. Eleven patients with various deletion sizes required tube feeding because of insufficient oral feeding associated with hypotonia, poorly coordinated swallowing, and/or gastroesophageal reflux. Gastrostomy was performed in two patients with the largest and the second largest deletions because of persistent insufficient oral feeding, failure to thrive regardless of tube feeding, recurrent respiratory distress, hypoglycemia, and/or carnitine deficiency.

Congenital heart defects were seen in 19/22 patients (86%). Three patients without heart defects had smaller deletions of 2.93, 5.49, and 7.51 Mb. The observed heart defects were common types,

TABLE I. Summary of Molecular-Cytogenetic Analysis of 22 WHS Patients

		Array-CGH analysis						
Patient no.	G-Banded chromosomes	Location and minimal deletion size of 4p		Distal breakpoint from 4pter[a]	Proximal breakpoint from 4pter	Other unbalanced region and minimal size	Final 4p rearrangement studied with a-CGH and FISH	Inheritance
1	46,XX	4p16.3	2.06 Mb	1–(63,075)	2,061,942–2,071,068	dup(10)(q26.3), 772 kb	Unbalanced translocation der(4) t(4;10)(p16.3,q26.3)	
2	46,XX	4p16.3	2.29 Mb	1–(41,413)	2,294,435–2,313,104		Isolated terminal	
3	add(4)(p16)	4p16.3	2.93 Mb	1–(63,075)	2,934,119–2,941,688	dup(4)(q31.22q35.2), 45.6 Mb	der(4)(4qter→q31.22:p16.3→qter)	
4	46,XX	4p16.3p16.2	3.45 Mb	1–(63,075)	3,453,423–3,475,088		Isolated terminal	
5	46,XX	4p16.3p16.1	5.26 Mb	1–(63,075)	5,259,705–5,286,063		Isolated terminal	
6	del(4)(p16.1)	4p16.3p16.1	5.49 Mb	1–(33,860)	5,488,869–5,517,610		Isolated terminal	De novo
7	del(4)(p16.1)	4p16.3p16.1	6.92 Mb	1–(33,860)	6,920,095–6,944,615		Isolated terminal	
8	del(4)(p16.1)	4p16.3p16.1	7.51 Mb	1–(63,075)	7,509,074–7,525,657		Isolated terminal	
9	del(4)(p15.3p16)	4p16.3p16.1	8.09 Mb	1–(63,075)	8,089,462–8,126,238		Isolated terminal	
10	add(4)(p15.3)	4p16.3p16.1	8.77 Mb	1–(63,075)	8,772,114–9,414,321		Isolated terminal	
11	add(4)(p15.2)	4p16.3p16.1	8.77 Mb	1–(33,860)	8,772,114–9,414,321	dup(8)(p23.3p23.1), 6.9 Mb	Unbalanced translocation der(4) t(4:8)(p16.1;p23.1)	Maternal
12	del(4)(p16.1)	4p16.3p16.1	8.77 Mb	1–(33,860)	8,772,114–9,414,321		Isolated terminal	De novo
13	add(4)(p15.3)	4p16.3p16.1	8.85 Mb	1,329,023–1,370,178	10,219,850–10,254,956		Isolated interstitial	
14	add(4)(p15.2)	4p16.3p15.33	11.11 Mb	1–(63,075)	11,105,238–11,129,635		Isolated terminal	De novo
15	46,XY,del(4)(p15.3p16.1)[26]/46,XY[4]	4p16.3p15.33	12.01 Mb	1–(33,860)	12,006,591–12,044,138		mos.del(4)(p15.33)/del(4)(p16.3)	
16	del(4)(p15.3)	4p16.3p15.33	12.33 Mb	1–(33,860)	12,331,994–12,371,059		Isolated terminal	De novo
17	del(4)(p15.32-p16.3)	4p16.3p15.33	13.63 Mb	813,367–841,095	14,467,735–14,498,501		Isolated interstitial	De novo
18	add(4)(p15.2)	4p16.3p15.32	15.70 Mb	1–(63,075)	15,700,625–15,737,006		Isolated terminal	
19	del(4)(p15.3)	4p16.3p15.31	18.62 Mb	1–(63,075)	18,616,970–18,655,860		Isolated terminal	De novo
20	del(4)(p15.2p16)	4p16.3p15.31	21.00 Mb	1–(63,075)	20,992,651–21,031,043	dup(11)(q25), 1.27 Mb	mos.der(4)t(4;11)(p15.31;q25)/del(4)(p15.31)	De novo
21	del(4)(p15.1)	4p16.3p15.1	28.35 Mb	1–(33,860)	28,348,051–28,384,613		Isolated terminal	De novo
22	del(4)(p15.1)	4p16.3p15.1	29.42 Mb	1–(63,075)	29,416,450–29,451,155		Isolated terminal	

Genomic locations of array results are according to NCBI build 36 (hg 18).
[a]Distal breakpoints of 41,413, 33,860, and 63,075 actually show terminal 4p deletions because the probes designed for the region are nonspecific to 4pter.

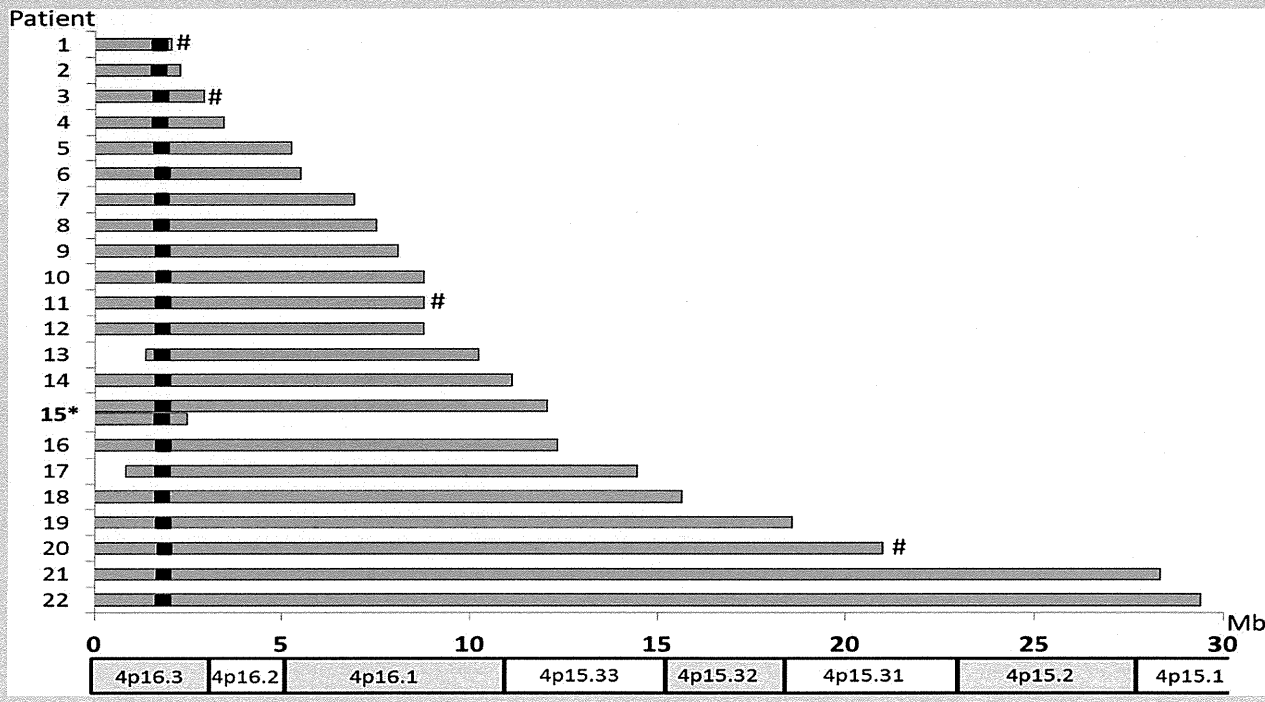

FIG. 1. Overview of 4p deletion sizes in each patient using chromosomal microarray analysis. Gray bars indicate deleted segments, black boxes indicate WHSCR2, and # denotes presence of other unbalanced regions. *Patient 15 has a mosaicism with another minor cell line of a smaller-sized terminal deletion determined by metaphase FISH.

including atrial septal defects in 13 patients, pulmonary stenosis in six, and patent ductus arteriosus in five. The severity of the heart defects was not correlated with deletion sizes or deleted regions. No life-threatening complex heart defects were present in this series.

Structural urogenital anomalies were detected in a total of 47% (9/19) patients, including renal hypoplasia or dysplasia in six. The prevalence of patients with renal hypoplasia or dysplasia was 0/3 (0%) in the small deletion-type, 3/11 (27%) in the intermediate, and 3/5 (60%) in the large. Renal hypoplasia or dysplasia resulted in renal failure in five patients (83%).

Ophthalmologic abnormalities were detected in a total of 62% patients (13/21). Strabismus and nasolacrimal obstruction were found in patients with small or intermediate deletion-types, whereas structural ocular anomalies were found in patients with intermediate (2/11, 18%) and large (3/5, 60%) deletion-types. The prevalence of cleft lip/palate was 32% (7/22), that of skeletal abnormalities was 45% (9/20), and that of hearing impairment was 55% (12/22).

Other complications included hypercholesterolemia (>220 mg/dl) in a total of 36% (5/14) patients in whom serum cholesterol levels were examined, and the hypercholesterolemia was not familial in all the patients except one, whose parental information was not available. Multiple osteochondromatosis was observed in Patient 2 with a terminal 2.29 Mb deletion. The age of onset of osteochondromatosis was around 2 years. Radiological examination revealed a cartilage-capped bony growth arising from the area of the growth palate of the distal tibia and from the surface of the scapula. The patient underwent several surgical resections for progressive osteochondromatosis. Direct sequencing and multiplex ligation-dependent probe amplification analysis of *EXT1* and *EXT2*, the genes responsible for multiple osteochondromatosis (multiple exostosis type I (OMIM#133700) and type II (OMIM#133701), respectively) [Francannet et al., 2001], showed no pathogenic sequence variants.

DISCUSSION

In the current study, we performed microarray and FISH-based molecular-cytogenetic investigations of 22 Japanese patients with WHS, coupled with a detailed and comprehensive clinical evaluation. This resulted in identification of previously unreported complex chromosomal mosaicism and implication of several findings about the genotype–phenotype correlation including severity of seizures and structural anomalies.

Unbalanced translocations combined with a 4p deletion or other complicated rearrangement were identified in a total of four (18%) patients, which was lower than the recently reported frequency of 45% (15/33) by South et al. [2008c]. This discrepancy might be attributable to selection bias in both studies or the possible presence of a translocation with acrocentric p-arm in the current study, which could be detected through silver staining of the nucleolar organizing region (NOR), FISH using alpha satellite DNA probes, or parental FISH studies using a WHS-specific 4p16.3 probe [South et al., 2008c].

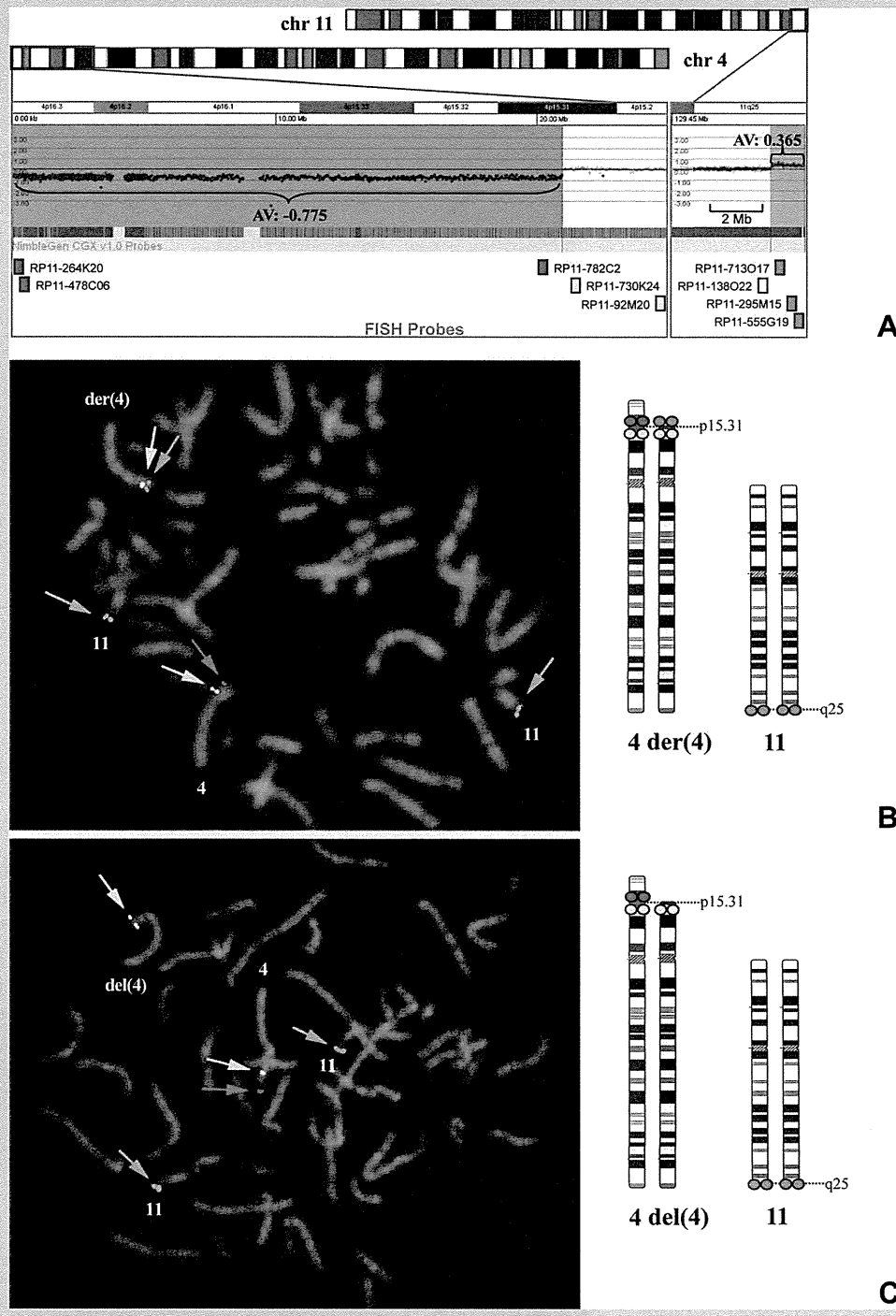

FIG. 2. Molecular-cytogenetic investigations of Patient 20. A: Upper panel shows microarray results. Whereas a 21.0-Mb copy number loss of 4pter with an average $\log_2$ value of −0.775 does not show a mosaicism, a 1.27-Mb copy number gain of 11qter with an average $\log_2$ value of 0.365 suggests a mosaicism. Lower panel shows BAC probes used in metaphase FISH. 4p probes deleted in both cell lines are shown in red, 11q probes duplicated in only the der(4)t(4;11) cell line are shown in green, and adjacent probes not deleted or duplicated in either cell line are shown in yellow at 4p or white at 11q. B: Metaphase FISH analysis showing the der(4)t(4;11) cell line. C: Metaphase FISH analysis showing the del(4) cell line. RP11-264K20 probe is shown in red, that for RP11-92M20 in yellow, and that for RP11-296M15 in green.

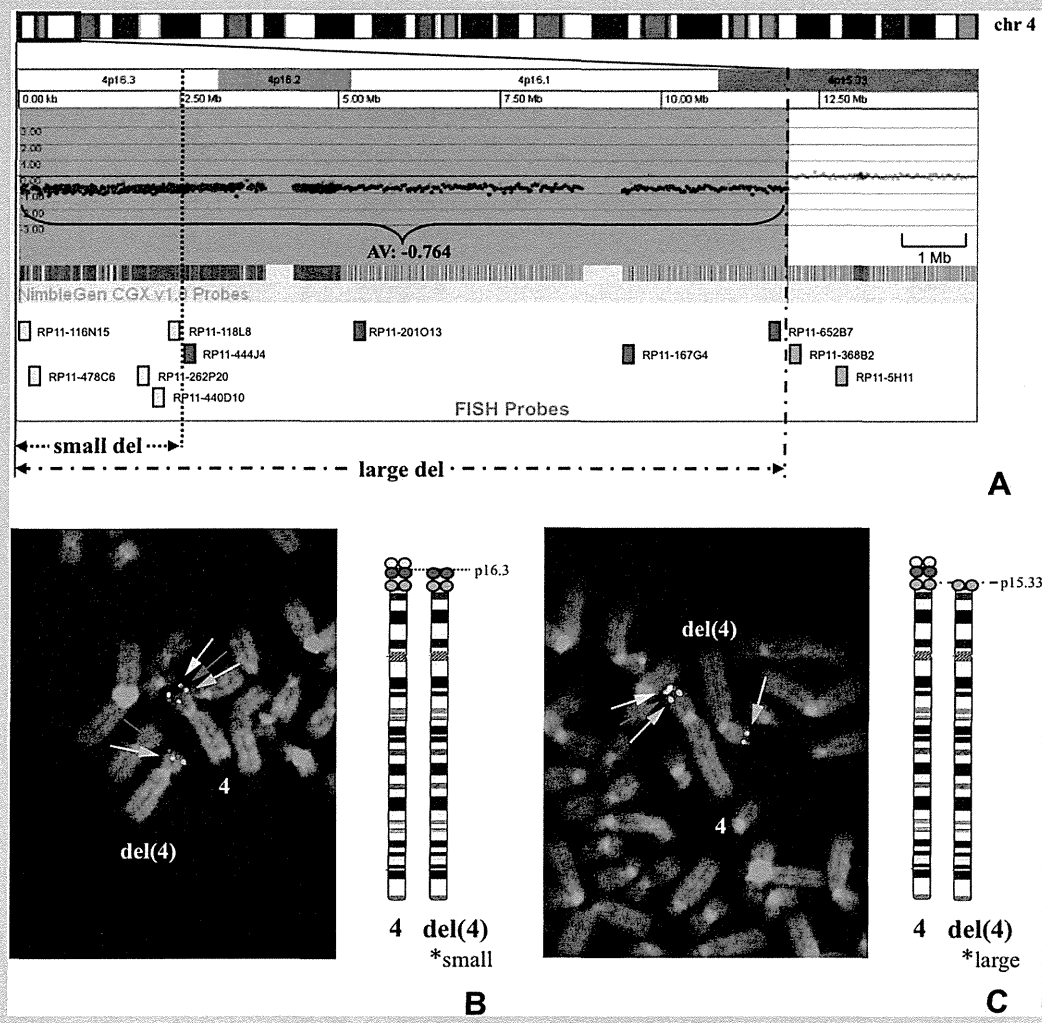

FIG. 3. Molecular-cytogenetic investigations of Patient 15. A: Upper panel shows microarray results. A 15-Mb copy number loss with an average $\log_2$ value of −0.764 does not suggest a mosaicism. Lower panel shows BAC probes used in metaphase FISH. Those deleted in both cell lines are shown in yellow, those deleted only in the cell line of the larger deletion are shown in red, and those not deleted in either cell line are shown in green. B: Metaphase FISH analysis showing the del(4)(p16.3) (2.48–2.66 Mb deletion) cell line. C: Metaphase FISH analysis showing the del(4)(p15.33) (11.9–12.1 Mb deletion) cell line. RP11-116N15 probe is shown in yellow that for RP11-118L8 in red, and that for RP11-652B7 in green.

Hitherto unreported patterns of complex mosaicism for two different structurally abnormal cell lines were identified in two of the patients in our current series using a combination of G-banding, microarray, and metaphase FISH analysis. Only a limited number of mosaicism cases have been previously reported of two cell lines both carrying 46 chromosomes and different structurally abnormal chromosomes, including del(8p)/inv dup del(8p) in several patients [Vermeesch et al., 2003; Pramparo et al., 2004; Hand et al., 2010]. Only one WHS patient was reported to carry two different structurally abnormal cell lines, del(4)(p16)/der(4)(qter-q31.3::pter–qter), which might have resulted from a meiotic crossing over event causing the der(4) cell line to be associated with a pericentric inversion and subsequent mitotic breakage [Syrrou et al., 2001]. A previous report showed expansion of a 4p terminal deletion between a mother and a son [Faravelli et al., 2007] and a subsequent report described this on 18q [South et al., 2008b]. Patient 15 might be another example of apparent instability of a terminal deletion, representing the expansion of a deletion within an individual rather than between generations.

Mosaicism of two different structurally abnormal cell lines, del(4)(p15.31)/der(4)t(4;11)(p15.31;q25), was indicated in Patient 20 by microarray through the lower $\log_2$ ratio of the duplicated 11q region. This supports the utility of microarray in that it can detect not only small copy number variation at a significantly higher resolution, but also detect mosaicism by incomplete $\log_2$ ratio compared with complete deletion or duplication [Ballif et al., 2006]. By contrast, mosaicism could not be detected in Patient 15 by microarray, perhaps because of the different levels of mosai-

TABLE II. Summary of Clinical Features in 22 WHS Patients

Patient no.	Age/sex	Minimal deletion sizes in 4p(Mb)	Accompanied duplicated regions	Seizure onset	Status epilepticus	Treatment at the time of this study/course of seizures	CNS complications	Developmental delay
1	6y/F	2.06	dup(10q),772 kb	+/9m	−	CZP/disappeared	−	Moderate (DQ41)/walk at 2y3m
2	13y/F	2.29		+/2y6m	−	VPA/disappeared for 5 years	N.I.	Severe (IQ23)/walk at 7y
3	1y8m/F	2.93	dup(4q),45.6 Mb	+/1y3m	−	−/disappeared after only one attack	−	Severe/no sitting
4	4y3m/F	3.45		+/7m	+	VPA, CLB/occurred frequently	Periventricular leukomalacia	Severe/no head control
5	5y10m/F	5.26		+/1y1m	−	CZP/well-controlled	N.I.	Moderate/walk at 4y
6	16y/F	5.49		+/2y1m	−	DZP/disappeared since 8y	N.I.	Severe/walk at 7y
7	18y/F	6.92		+/6m	+	VPA, Br, Vit B6 (West syndrome)/improved after Br at 1y	−	Severe (IQ10)/walk at 7y
8	6y6m/M	7.51		+/7m	+	TPM, PB, CLB, Br/improved after Br at 3y	N.I.	Severe/roll over at 1y5m
9	5y3m/F	8.09		+/10m	+	PB, VPA/occurred frequently	−	Severe/head control at 12m
10	7m/M	8.77		−	−	−/−	−	Severe
11	8y/F	8.77	dup(8p),6.9 Mb	+/6m	+	VPA, PB/improved after 2y	−	Severe (DQ10)/sit at 4y
12	16y/F	8.77		+/7m	+	VPA, PHT/improved after 2y	Ventricular enlargement	Severe/head control at 2y
13	12y/F	8.85 (1.37–10.22)			−	−/−	−	Moderate/walk at 2y3m
14	5y/F	11.11		+/9m	+	VPA, Br/well-controlled	−	Severe/walk
15	9m/M	12.02		+/8m	+	VPA/continued	Ventricular enlargement	Severe
16	1y11m/F	12.33		+/9m	+	VPA, LGT, CZP/occurred frequently	HCC, Cerebellar atrophy	Severe (DQ30)/head control at 9m
17	18y/F	13.63 (0.84–14.5)		+/1y	+	−/disappeared for several years	HCC	Severe (IQ10)/walk at 5y
18	3y/F	15.70		+/1y2m	+	VPA, CLB, Br/improved gradually	−	Severe/head control
19	2y11m/F	18.60		+/2m	+	PB, CZP, TPM/occurred frequently	−	Severe/no head control
20	4y/F	21.00	dup(11q),1.27 Mb	+/1m	−	VPA, ZNS/disappeared for two years	Cerebral atrophy	Severe/no head control
21	2y10m/F	28.35		+/11m	+	TPM, CLB/disappeared since 2y	Cerebral atrophy	Severe
22	6y/M	29.42		+/2m	+	VPA, ESM, PB/occurred frequently	HCC, Grey matter heterotopia, white matter volume loss	Severe (DQ10)/no head control

Patient no.	Height/weight (SD)[a]	Feeding	CL/CP	Heart	Urogenital	Skeletal	Ophthalmologic	Hearing impairment	Other complication(s)
1	−2.4/−2.0	Oral	−	ASD	−	−	Strabismus	−	
2	−5.4/−3.5	Oral	−	ASD	N.I.	Scoliosis (mild)	−	−	Multiple osteochondromatosis
3	−5.3/−2.3	Tube	−	−	−	−	−	Severe	hypercholesterolemia
4	−4.3/−3.0	Tube	−	ASD, PDA, VSD	N.I.	Limited hip flexion	Strabismus	Moderate	
5	−3.8/−2.9	Oral	−	ASD	N.I.	−	Strabismus	−	Hypercholesterolemia
6	−4.9/−3.0	Oral	−	−	−	N.I.	Strabismus (ET)	−	
7	−5.1/−2.5	Oral	−	PS	Renal hypoplasia, RF	Pes planus	−	Moderate	Hypercholesterolemia, hyperuricemia
8	−6.4/−3.7	Tube	−	−	−	−	NDO	Moderate	Fanconi syndrome due to VPA
9	−5.8/−4.1	Oral	−	ASD, PS	−	−	Strabismus	Moderate	
10	−4.5/−3.9	Tube	+ (CP)	PDA	−	−	Right cataract	−	
11	−4.1/−3.3	Tube	+ (SMCP)	AR	−	N.I.	Strabismus, NDO	−	
12	−11.7/−5.3	Tube	+ (CL/CP)	PS	Renal hypoplasia, RF	Scoliosis (mild)	Strabismus (XT)	Severe	
13	−3.0/−2.3	Tube	−	VSD	−	−	−		
14	−5.2/−4.0	Oral		ASD	−	−	−	Moderate	
15	−2.0/−2.3	Oral	−	ASD, PS	Criptorchidism	−	N.I.	Moderate	
16	−3.4/−2.7	Tube	+ (SMCP)	ASD, PDA	Hydronephrosis	Talipes varus	Strabismus (XT), NDO	−	
17	−5.3/−3.8	Oral	−	ASD	Renal hypoplasia, RF	Acetabular dysplasia	Cataract	−	Hypercholesterolemia
18	−5.6/−4.0	Tube	−	ASD, PS	Renal hypoplasia, RF	Sagittal craniosynostosis	Coloboma	−	Hypercholesterolemia
19	−4.4/−2.4	Tube	−	ASD, PS	−	Scoliosis	Optic nerve atrophy	Moderate	
20	−3.3/−2.6	Tube	−	PDA, VSD	Renal hypoplasia VUR	−	−	Moderate	
21	−2.3/−3.1	GS	+(CP)	ASD, PDA	UJS, RF	Talipes varus Cervical spine abnormalities	−	Severe	
22	−1.3/−1.4	GS	+	ASD	Renal dysplasia, RF, cryptorchidism, hypospadias	−	Cataract, coloboma	Severe	

ASD, atrial septal defect; Br, potassium/sodium bromide; CL, cleft lip; CLB, clobazam; CNS, central nervous system; CP, cleft palate; CZP, clonazepam; DQ, developmental quotient; DZP, diazepam; ESM, ethosuximide; ET, esotropia; F, Female; GS, gastrostomy; HCC, hypoplasia of the corpus callosum; IQ, intelligence quotient; LGT, lamotrigine, M, Male; m, months; NDO, nasolacrimal duct obstruction; N.I., not investigated; PB, phenobarbital; PDA, patent ductus arteriosus; PHT, phenytoin; PS, pulmonary stenosis; RF, renal failure; SMCP, submucous cleft palate; TPM, topiramate; UJS, ureteropelvic junction stenosis; VPA, valproate; VSD, ventricular septal defect; VUR, vesicoureteric reflux; XT, exotropia; y, years; ZNS, zonisamide.

[a]Height and weight were evaluated at the time of this study.

TABLE III. Frequency of Major Structural Defects According to Deletion Sizes

	Small (<6 Mb)	Intermediate (6–15 Mb)	Large (>15 Mb)
Congenital heart defects	4/6 (67%)	10/11 (91%)	5/5 (100%)
Renal abnormalities [renal failure]	0/3 (0%) [0/3]	4/11 (36%) [3/11]	4/5 (80%) [3/5]
Ocular defects	0/6 (0%)	2/11 (18%)	3/5 (60%)
Cleft lip/palate	0/6 (0%)	5/11 (45%)	2/5 (40%)
Skeletal anomalies	2/6 (33%)	4/11 (36%)	3/5 (60%)

FIG. 4. Clinical photographs. Patient 1 at age 8 years and 10 months (A), Patient 2 at age 4 years (B), Patient 6 at age 18 years (C), Patient 7 at age 2 years and 2 months (D), Patient 8 at age 3 months (E), Patient 11 at age 8 years and 8 months (F), Patient 12 at age 1 year and 3 months (G), Patient 13 at age 6 years and 4 months (H), and Patient 16 at age 2 years and 3 months (I). Typical craniofacial features are present in all the patients except for Patient 1 (A) and Patient 13 (H), showing subtle features without the Greek warrior helmet appearance.

cism between the two patients: 22:8 in Patient 20 and 45:11 in Patient 15.

Our study included four patients with other duplicated chromosomal regions detected by microarray. The duplicated segment of 10q26.3–qter (772 kb) in Patient 1, 11q25–qter (1.27 Mb, mosaicism) in Patient 20, and 8p23.1–pter (6.9 Mb) in Patient 11 have not been reported to associate with extensive disease pathology in a trisomic state [Engelen et al., 2000; Harada et al., 2002; Iwanowski et al., 2011]. The 45.6 Mb duplication at the 4q31.22–qter region in Patient 3 is considered to be mainly associated with psychomotor delay and often with cardiac and renal anomalies [Otsuka et al., 2005; Wang et al., 2009]. Indeed, Patient 3 showed severe developmental delay in spite of a small 4p deletion (2.93 Mb), but no apparent cardiac or renal anomaly.

The severity of seizures is evaluated from the time of onset and the presence of status epilepticus. Six patients with small deletions (<6 Mb) from 4pter tended to have a later onset of seizures and status epilepticus was less common than those patients with intermediate (6–15 Mb) or large deletions (>15 Mb). Developmental delay was severe in most patients, with the exception of three with a moderate delay: two of these had small terminal deletions (2.06 and 5.26 Mb) and one had an intermediate interstitial deletion (8.85 Mb). Seizure severity is, therefore, suggested to correlate with the 4p deletion size, which might result in correlation between severity of developmental delay and the 4p deletion size.

Candidate region(s) for seizures in patients with WHS and possible responsible genes are shown in Figure 5. Although *LETM1* is presently considered to be the major responsible gene for seizures [Endele et al., 1999; Rauch et al., 2001; South et al., 2007], the more distal region of the chromosome has also been suggested as a candidate region for seizure penetrance [South et al., 2008a; Misceo et al., 2012]. Indeed, Patient 13 in our series did not have seizures and had an interstitial deletion (1.37–10.22 Mb from 4pter) encompassing *LETM1* but preserving the distal regions, which is similar to "Case 6" reported by Maas et al. [2008] with an interstitial deletion (1.3–2.5 Mb) including *LETM1* and no seizures. Four patients with seizures were reported to have small distal 4p deletions not including *LETM1* [Faravelli et al., 2007; Maas et al., 2008; Zollino et al., 2008; Misceo et al., 2012]. Considering a patient with ring chromosome 4 and a 4p terminal deletion of 760 kb not experiencing seizures [Concolino et al., 2007], the susceptible gene(s) for seizures in WHS might be localized in the region between 760 kb and 1.3 Mb from the 4pter. In our series, Patient 17 with an interstitial deletion

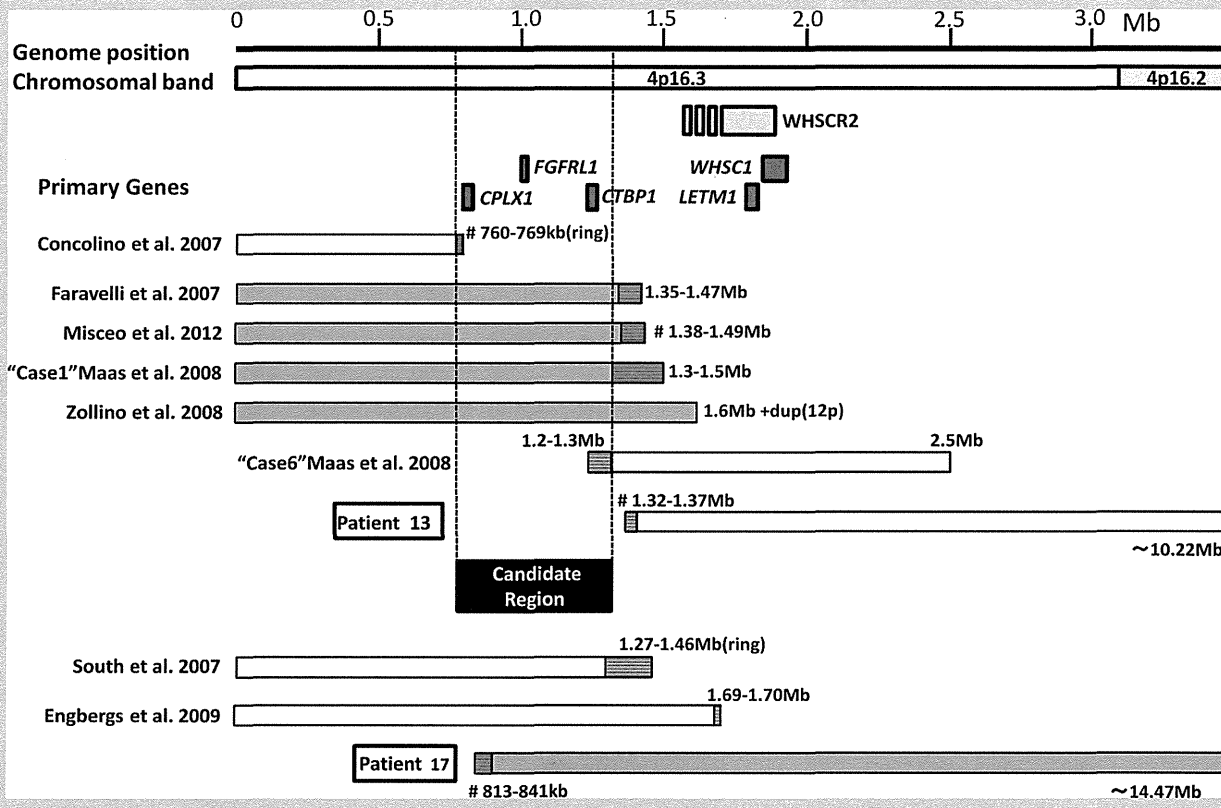

FIG. 5. Schema showing candidate region(s) for the occurrence of seizures [Genome coordinates hg18]. A new candidate region is suggested between 0.76 and 1.3 Mb from 4pter, encompassing *CTBP1* and *CPLX1*, and distal to the previously-supposed candidate gene *LETM1*. White bars indicate deleted segments in patients without seizures. Light gray bars indicate deleted segments in those with seizures. Bars with horizontal stripes indicate deletion breakpoints with variation according to probe-gaps. # Represents patients in whom the breakpoint was determined by oligonucleotide microarray, while breakpoints in the other patients were determined by BAC array or FISH using BAC probes.

encompassing both *LETM1* and most of the new candidate region had severe seizures.

CTBP1 and *CPLX1* are localized in this new susceptible region for seizures. *CTBP1* encodes a transcriptional corepressor that acts at the promoters of many genes [Chinnadurai, 2007]. In an epileptogenic rat model, a ketogenic diet as well as 2-deoxy-D-glucose, a glycolysis-inhibiting drug, reduces epilepsy by stimulating Ctbp activity. Ctbp co-operates with transcriptional factor NRSF to repress expression of BDNF, a strongly suspected epileptogenic signaling molecule [Garriga-Canut et al., 2006]. The hemizygosity of *CTBP1* in WHS patients is therefore considered a potential contributor to the progression of epilepsy [Simon and Bergemann, 2008]. *CPLX1* encodes a type of complexin that binds to syntaxin within the SNARE complex and regulates the fusion of synaptic vesicles [McMahon et al., 1995]. Homozygous *Cplx1* deletion mutant mice develop strong ataxia and sporadic seizures [Reim et al., 2001; Glynn et al., 2005]. These findings suggest that *CTBP1* and *CPLX1* as well as *LETM1* could be susceptibility genes for seizures in WHS.

Bromide therapy was previously reported to be an effective antiepileptic drug in four patients with WHS, in whom it was shown to reduce status epilepticus [Kagitani-Shimono et al., 2005]. In the current study, four patients were administered bromide therapy, which was effective in all. In particular, Patients 7 and 8 showed a marked reduction in seizure frequency after the initiation of bromide therapy. Further information including the types or severity of seizures, electroencephalography (EEG) patterns, efficacy of treatment, and microarray-based deletion mapping in a larger patient series will be necessary to establish a detailed seizure phenotype–genotype correlation.

Hypercholesterolemia, which has not been reported in previous studies, was observed in five patients in the present study, suggesting it to be a noteworthy complication of WHS. *LRPAP1*, localized 3.5 Mb from 4pter, was deleted in four of the patients. *LRPAP1* encodes LDL receptor-related protein-associated protein 1 that plays an important role in lipoprotein metabolism [Willnow et al., 1995], and might therefore be related to hypercholesterolemia. Multifactorial inheritance, including nutritional problems, could also be related to the occurrence of hypercholesterolemia.

In conclusion, this genotype–phenotype correlation study using microarray and FISH-based molecular-cytogenetic investigations uncovered chromosomal rearrangements in all patients including previously unreported complex chromosomal mosaicism. It also demonstrated the correlation of deletion size from 4pter with seizure severity and with occurrence of renal hypoplasia/dysplasia and structural ocular anomalies, and described additional clinical features including hypercholesterolemia. Moreover, a new susceptible region distal to the previously-supposed candidate gene *LETM1* was suggested for the occurrence of seizures, and the usefulness of bromide therapy was stressed for seizure management. To prevent intractable seizures and status epileptics, patients with 4p deletion involving the new susceptible region as well as *LETM1* are recommended to have careful EEG follow-up and intensive pharmacological treatment based on the seizure occurrence and EEG findings, including application of bromide therapy. These findings are relevant to the improvement of WHS healthcare guidelines, as well as to the elucidation of gene(s) function in the deleted region.

ACKNOWLEDGMENTS

We thank the patients and their families for participating in this study. This work was supported by Research on Intractable Diseases from Japanese Ministry of Health, Labour and Welfare (K.T., Y.F.).

REFERENCES

Ballif BC, Rorem EA, Sundin K, Lincicum M, Gaskin S, Coppinger J, Kashork CD, Shaffer LG, Bejjani BA. 2006. Detection of low-level mosaicism by array CGH in routine diagnostic specimens. Am J Med Genet Part A 140A:2757–2767.

Battaglia A, Carey JC, Cederholm P, Viskochil DH, Brothman AR, Galasso C. 1999. Natural history of Wolf–Hirschhorn syndrome: Experience with 15 cases. Pediatrics 103:830–836.

Battaglia A, Filippi T, Carey JC. 2008. Update on the clinical features and natural history of Wolf–Hirschhorn (4p-) syndrome: Experience with 87 patients and recommendations for routine health supervision. Am J Med Genet Part C 148C:246–251.

Battaglia A, Filippi T, South ST, Carey JC. 2009. Spectrum of epilepsy and electroencephalogram patterns in Wolf–Hirschhorn syndrome: Experience with 87 patients. Dev Med Child Neurol 51:373–380.

Catela C, Bilbao-Cortes D, Slonimsky E, Kratsios P, Rosenthal N, Te Welscher P. 2009. Multiple congenital malformations of Wolf–Hirschhorn syndrome are recapitulated in Fgfrl1 null mice. Dis Model Mech 2:283–294.

Chinnadurai G. 2007. Transcriptional regulation by C-terminal binding proteins. Int J Biochem Cell Biol 39:1593–1607.

Concolino D, Rossi E, Strisciuglio P, Iembo MA, Giorda R, Ciccone R, Tenconi R, Zuffardi O. 2007. Deletion of a 760 kb region at 4p16 determines the prenatal and postnatal growth retardation characteristic of Wolf–Hirschhorn syndrome. J Med Genet 44:647–650.

Endele S, Fuhry M, Pak SJ, Zabel BU, Winterpacht A. 1999. LETM1, a novel gene encoding a putative EF-hand Ca(2+)-binding protein, flanks the Wolf–Hirschhorn syndrome (WHS) critical region and is deleted in most WHS patients. Genomics 60:218–225.

Engbers H, van der Smagt JJ, van 't Slot R, Vermeesch JR, Hochstenbach R, Poot M. 2009. Wolf–Hirschhorn syndrome facial dysmorphic features in a patient with a terminal 4p16.3 deletion telomeric to the WHSCR and WHSCR 2 regions. Eur J Hum Genet 17:129–132.

Engelen JJ, Moog U, Evers JL, Dassen H, Albrechts JC, Hamers AJ. 2000. Duplication of chromosome region 8p23.1→p23.3: A benign variant? Am J Med Genet 91:18–21.

Faravelli F, Murdolo M, Marangi G, Bricarelli FD, Di Rocco M, Zollino M. 2007. Mother to son amplification of a small subtelomeric deletion: A new mechanism of familial recurrence in microdeletion syndromes. Am J Med Genet Part A 143A:1169–1173.

Francannet C, Cohen-Tanugi A, Le Merrer M, Munnich A, Bonaventure J, Legeai-Mallet L. 2001. Genotype–phenotype correlation in hereditary multiple exostoses. J Med Genet 38:430–434.

Garriga-Canut M, Schoenike B, Qazi R, Bergendahl K, Daley TJ, Pfender RM, Morrison JF, Ockuly J, Stafstrom C, Sutula T, Roopra A. 2006. 2-Deoxy-D-glucose reduces epilepsy progression by NRSF-CtBP-dependent metabolic regulation of chromatin structure. Nat Neurosci 9:1382–1387.

Glynn D, Drew CJ, Reim K, Brose N, Morton AJ. 2005. Profound ataxia in complexin I knockout mice masks a complex phenotype that includes exploratory and habituation deficits. Hum Mol Genet 14:2369–2385.

Hand M, Gray C, Glew G, Tsuchiya KD. 2010. Mild phenotype in a patient with mosaic del(8p)/dup del/inv (8p). Am J Med Genet Part A 152A:2827–2831.

Harada N, Takano J, Kondoh T, Ohashi H, Hasegawa T, Sugawara H, Ida T, Yoshiura K, Ohta T, Kishino T, Kajii T, Niikawa N, Matsumoto N. 2002. Duplication of 8p23.2: A benign cytogenetic variant? Am J Med Genet 111:285–288.

Hirschhorn K, Cooper HL, Firschein IL. 1965. Deletion of short arms of chromosome 4–5 in a child with defects of midline fusion. Humangenetik 1:479–482.

Iwanowski PS, Panasiuk B, Van Buggenhout G, Murdolo M, Mysliwiec M, Maas NM, Lattante S, Korniszewski L, Posmyk R, Pilch J, Zajaczek S, Fryns JP, Zollino M, Midro AT. 2011. Wolf–Hirschhorn syndrome due to pure and translocation forms of monosomy 4p16.1→pter. Am J Med Genet Part A 155A:1833–1847.

Izumi K, Okuno H, Maeyama K, Sato S, Yamamoto T, Torii C, Kosaki R, Takahashi T, Kosaki K. 2010. Interstitial microdeletion of 4p16.3: Contribution of WHSC1 haploinsufficiency to the pathogenesis of developmental delay in Wolf–Hirschhorn syndrome. Am J Med Genet Part A 152A:1028–1032.

Jiang D, Zhao L, Clapham DE. 2009. Genome-wide RNAi screen identifies Letm1 as a mitochondrial Ca^{2+}/H^{+} antiporter. Science 326:144–147.

Kagitani-Shimono K, Imai K, Otani K, Kamio N, Okinaga T, Toribe Y, Suzuki Y, Ozono K. 2005. Epilepsy in Wolf–Hirschhorn syndrome (4p-). Epilepsia 46:150–155.

Maas NM, Van Buggenhout G, Hannes F, Thienpont B, Sanlaville D, Kok K, Midro A, Andrieux J, Anderlid BM, Schoumans J, Hordijk R, Devriendt K, Fryns JP, Vermeesch JR. 2008. Genotype–phenotype correlation in 21 patients with Wolf–Hirschhorn syndrome using high resolution array comparative genome hybridisation (CGH). J Med Genet 45:71–80.

McMahon HT, Missler M, Li C, Sudhof TC. 1995. Complexins: Cytosolic proteins that regulate SNAP receptor function. Cell 83:111–119.

Misceo D, Baroy T, Helle JR, Braaten O, Fannemel M, Frengen E. 2012. 1.5Mb deletion of chromosome 4p16.3 associated with postnatal growth delay, psychomotor impairment, epilepsy, impulsive behavior and asynchronous skeletal development. Gene 507:85–91.

Nimura K, Ura K, Shiratori H, Ikawa M, Okabe M, Schwartz RJ, Kaneda Y. 2009. A histone H3 lysine 36 trimethyltransferase links Nkx 2–5 to Wolf–Hirschhorn syndrome. Nature 460:287–291.

Otsuka T, Fujinaka H, Imamura M, Tanaka Y, Hayakawa H, Tomizawa S. 2005. Duplication of chromosome 4q: Renal pathology of two siblings. Am J Med Genet Med A 134A:330–333.

Pramparo T, Giglio S, Gregato G, de Gregori M, Patricelli MG, Ciccone R, Scappaticci S, Mannino G, Lombardi C, Pirola B, Giorda R, Rocchi M, Zuffardi O. 2004. Inverted duplications: How many of them are mosaic? Eur J Hum Genet 12:713–717.

Rauch A, Schellmoser S, Kraus C, Dorr HG, Trautmann U, Altherr MR, Pfeiffer RA, Reis A. 2001. First known microdeletion within the Wolf–Hirschhorn syndrome critical region refines genotype–phenotype correlation. Am J Med Genet 99:338–342.

Reim K, Mansour M, Varoqueaux F, McMahon HT, Sudhof TC, Brose N, Rosenmund C. 2001. Complexins regulate a late step in Ca^{2+}-dependent neurotransmitter release. Cell 104:71–81.

Rodriguez L, Zollino M, Climent S, Mansilla E, Lopez-Grondona F, Martinez-Fernandez ML, Murdolo M, Martinez-Frias ML. 2005. The new Wolf–Hirschhorn syndrome critical region (WHSCR-2): A description of a second case. Am J Med Genet Part A 136A:175–178.

Simon R, Bergemann AD. 2008. Mouse models of Wolf–Hirschhorn syndrome. Am J Med Genet Part C 148C:275–280.

South ST, Bleyl SB, Carey JC. 2007. Two unique patients with novel microdeletions in 4p16.3 that exclude the WHS critical regions: Implications for critical region designation. Am J Med Genet Part A 143A:2137–2142.

South ST, Hannes F, Fisch GS, Vermeesch JR, Zollino M. 2008a. Pathogenic significance of deletions distal to the currently described Wolf–Hirschhorn syndrome critical regions on 4p16.3. Am J Med Genet Part C 148C:270–274.

South ST, Rope AF, Lamb AN, Aston E, Glaus N, Whitby H, Maxwell T, Zhu XL, Brothman AR. 2008b. Expansion in size of a terminal deletion: A paradime shift for parental follow-up studies. J Med Genet 45:391–395.

South ST, Whitby H, Battaglia A, Carey JC, Brothman AR. 2008c. Comprehensive analysis of Wolf–Hirschhorn syndrome using array CGH indicates a high prevalence of translocations. Eur J Hum Genet 16:45–52.

Syrrou M, Borghgraef M, Fryns JP. 2001. Unusual chromosomal mosaicism in Wolf–Hirschhorn syndrome: del(4)(p16)/der(4)(qter-q31.3::pter-qter). Am J Med Genet 104:199–203.

Vermeesch JR, Thoelen R, Salden I, Raes M, Matthijs G, Fryns JP. 2003. Mosaicism del(8p) inv dup/(8p) in dysmorphic a female infant: A mosaic formed by a meiotic error at the 8p gene OR an independent terminal deletion event. J Med Genet 40e:93.

Wang JC, Fisker T, Dang L, Teshima I, Nowaczyk MJ. 2009. 4.3-Mb triplication of 4q32.1–q32.2: Report of a family through two generations. Am J Med Genet Part A 149A:2274–2279.

Willnow TE, Armstrong SA, Hammer RE, Herz J. 1995. Functional expression of low density lipoprotein receptor-related protein is controlled by receptor-associated protein in vivo. Proc Natl Acad Sci USA 92:4537–4541.

Wolf U, Reinwein H, Porsh R, Schroter R, Baitsch H. 1965. Defizienz am den kurze Armen eines chromosomes nr.4. Humnangenetik 1:397–413.

Wright TJ, Ricke DO, Denison K, Abmayr S, Cotter PD, Hirschhorn K, Keinanen M, McDonald-McGinn D, Somer M, Spinner N, Yang-Feng T, Zackai E, Altherr MR. 1997. A transcript map of the newly defined 165 kb Wolf–Hirschhorn syndrome critical region. Hum Mol Genet 6:317–324.

Zollino M, Di Stefano C, Zampino G, Mastroiacovo P, Wright TJ, Sorge G, Selicorni A, Tenconi R, Zappala A, Battaglia A, Di Rocco M, Palka G, Pallotta R, Altherr MR, Neri G. 2000. Genotype–phenotype correlations and clinical diagnostic criteria in Wolf–Hirschhorn syndrome. Am J Med Genet 94:254–261.

Zollino M, Lecce R, Fischetto R, Murdolo M, Faravelli F, Selicorni A, Butte C, Memo L, Capovilla G, Neri G. 2003. Mapping the Wolf–Hirschhorn syndrome phenotype outside the currently accepted WHS critical region and defining a new critical region, WHSCR-2. Am J Hum Genet 72:590–597.

Zollino M, Murdolo M, Marangi G, Pecile V, Galasso C, Mazzanti L, Neri G. 2008. On the nosology and pathogenesis of Wolf–Hirschhorn syndrome: Genotype–phenotype correlation analysis of 80 patients and literature review. Am J Med Genet Part C 148C:257–269.

Congenital Anomalies
THE JAPANESE TERATOLOGY SOCIETY
doi:10.1111/cga.12004
Congenital Anomalies 2013; **53**, 67–72 67

ORIGINAL ARTICLE

Craniofacial and dental malformations in Costello syndrome: A detailed evaluation using multi-detector row computed tomography

Masashi Takahashi[1] and Hirofumi Ohashi[2]
[1]Department of Pediatric Dentistry, Nihon University Graduate School of Dentistry at Matsudo, Matsudo, and [2]Division of Medical Genetics, Saitama Children's Medical Center, Saitama, Japan

ABSTRACT **Costello syndrome is a rare multiple congenital anomaly syndrome caused by heterozygous germline *HRAS* mutations, which is characterized by intellectual disability, growth retardation, distinctive facies, loose skin, cardiomyopathy and a preposition to malignancies. Although teeth abnormalities have been encountered in nearly two-thirds of the patients in literature, the evaluation tended to be limited to the extent which can be obtained from physical examination. We investigated detailed craniofacial, oral and dental findings in four patients with Costello syndrome. In this study, images reconstructed by multi-detector row computed tomography (MDCT) were used as substitutes for dental cast study and panoramic and lateral cephalometric radiograph studies to evaluate dental arches, tooth size, relationships between craniofacial and dental structures, and hypodontia. All four patients showed true/relative macrocephaly with facial bone hypoplasia and gingival hypertrophy. Occlusal attrition, malocclusion, small dental arches, microdontia, and convex face were noted in three patients. In addition, one patient showed dental caries, conic tooth and gingivitis, and another patient showed hypodontia. Our study suggests that craniofacial and dental abnormalities are common in Costello syndrome patients and comprehensive dental care should be provided from early infancy. To our knowledge, this is the first study of thorough craniofacial and dental evaluation by using MDCT in Costello syndrome. MDCT is a useful tool for precise evaluation of craniofacial and oral manifestations in patients with congenital anomaly/intellectual disability syndromes.**

Key Words: cephalometric analysis, Costello syndrome, multi-detector row computed tomography, small dental arch, malocclusion

INTRODUCTION

Costello syndrome is a rare multiple congenital anomaly syndrome characterized by intellectual disability, growth retardation, distinctive facies, loose skin, cardiomyopathy and a preposition to malignancies (Hennekam 2003), the prevalence of which is estimated to be 1 in 1 290 000 (Abe et al. 2012). Costello syndrome is caused by heterozygous germline *HRAS* mutations (Aoki et al. 2005) and is listed as one of the RASopathies, a group of related disorders caused by germline mutations in the Ras/mitogen-activated protein kinase pathway, which includes Noonan syndrome, cardio-facio-cutaneous (CFC) syndrome, and Costello syndrome, with considerable phenotypic overlap among these disorders (Rauen et al. 2010).

Craniofacial and oral features previously reported in Costello syndrome include macrocephaly, prominent forehead, high-arched palate, macroglossia, gingival hypertrophy, malocclusion, enamel hypoplasia and caries (Der Kaloustian et al. 1991; Di Rocco et al. 1993; Teebi and Shaabani 1993; Zampino et al. 1993; Johnson et al. 1998; van Eeghen et al. 1999; Delrue et al. 2003; Hennekam 2003; Kawame et al. 2003). Although teeth abnormalities were encountered in nearly two-thirds of the patients in the comprehensive review by Hennekam et al. (2003), the evaluation tended to be limited to the extent that can be obtained from physical examination. We here report on the result of our investigation of detailed craniofacial, oral and dental findings in four patients with Costello syndrome by using multi-detector row computed tomography (MDCT).

MATERIALS AND METHODS

Patients

A total of four patients with Costello syndrome, two male and two female, ranging in age between 5 and 7 years, were included in this study. All four patients were identified as having a missense mutation in the *HRAS* gene; c.34G>A (p.Gly12Ser) in patients 1, 2 and 3, and c.38G>A (p.Gly13Asp) in patient 4, either in exon 2. Clinical manifestations of the four patients are shown in Table 1. This study protocol was approved by the Ethics Committee of Saitama Children's Medical Center and proper informed consent was obtained from the legal guardians of patients.

Oral, dental, and craniofacial studies

Intraoral features such as palatal morphology, tooth calcification, occlusion and tooth eruption status were evaluated on physical examination. In addition, images reconstructed by MDCT were used as substitutes for dental cast study and panoramic and lateral cephalometric radiograph studies to evaluate the dental arches, tooth size, relationships between craniofacial and dental structures, and hypodontia. The following MDCT imaging conditions were used: window width, 1500; and window level, 450 (Hirai et al. 2010, 2011; Yamauchi et al. 2010). Crown and dental arch sizes were measured using Image J with a resolution accuracy of 0.1 mm. Lateral cephalometric analysis was performed based on the method developed by Iizuka and Ishikawa (1957). To perform cephalometric measurements, we made adjustments by rotating the mandibular bone image toward the expected actual intercuspal position. All measured data in this study were compared with standard values for

Correspondence: Masashi Takahashi, Department of Pediatric Dentistry, Nihon University Graduate School of Dentistry at Matsudo, 2-870-1 Sakaecho-Nishi, Matsudo, Chiba 271-8587, Japan. Email: matakahashidentist@yahoo.co.jp
Received September 24, 2012; revised and accepted November 4, 2012.

Table 1 Clinical manifestations of four patients with Costello syndrome

Patients	1	2	3	4
Gender	M	M	F	F
Age (years)	5	6	6	7
Intellectual disability	+ (Severe)	+	+	+
Height (SD)	−6.8	−5.9	−4.9	−2.7
Head circumference (SD)	−2.5	+0.27	+0.29	+2.9
Distinctive facies	+	+	+	+
Cardiac defect	HCM, AT	HCM, AT, VSD, MR	−	HCM, AT
Skeletal abnormality	HD, FD	HD, FD	HD, FD	FD
Neoplasia	−	−	−	−
Other	Tracheomalacia	Inguinal hernia	Exotropia	GHD
HRAS mutation	c.34G>A (p.G12S)	c.34G>A (p.G12S)	c.34G>A (p.G12S)	c.38G>A (p.13G>D)

+, present; −, absent; AT, atrial tachycardia; F, female; FD, foot deformity; GHD, growth hormone deficiency; HCM, hypertrophic cardiomyopathy; HD, hip dislocation; M, male; MR, mitral regurgitation; VSD, ventricular septal defect.

Japanese individuals (Iizuka and Ishikawa 1957; Otsubo 1964; Kato 1979; Fukawa 2008).

RESULTS

Oral and dental features noted in four patients are summarized in Table 2. On physical examination, all four patients had open mouth, thick lips and gingival hypertrophy. Other common features noted in all but one patient were occlusal attrition (patients 1, 2, 3), high-arched palate (patients 2,3,4) and malocclusion (patients 1 and 4 exhibited open bite, and patient 3 cross bite). In addition, one patient (patient 4) exhibited dental caries in a single tooth, a single conic tooth, and gingivitis. Enamel hypoplasia, an occasionally reported feature in patients with Costello syndrome, was not apparent in any of our patients (Fig. 1). Crowding of teeth was also not observed in the four patients. Panolamic images reconstructed with MDCT revealed a congenital tooth defect (mandibular left second premolar) in one patient (patient 3; Fig. 2).

Small dental arch was present in all patients except patient 1 (Table 3). Morphological categorization of small dental arches in the three patients were as follows: one patient (patient 2) exhibited U-shaped dental arch in the maxilla and narrow dental arch in the mandible; and two patients (patients 3 and 4) showed narrow dental arch in the maxilla and rectangular dental arch in the mandible (Fig. 3).

In terms of tooth size, maxillary teeth, especially lateral incisors and first and second molars in primary teeth and first molar in permanent teeth, tend to be small in these patients studied (Table 4). The degree of smallness of the maxillary teeth was most marked in the second molars in primary teeth of the two male patients (patients 1 and 2).

Cephalometric analysis (Table 5) revealed that, among the four patients studied, a convex face (increased facial convexity) was present in three patients (patients 1, 2 and 3), associated with maxillary overhang (increased SNA angle) observed in one patient (Patient 1), and with mandibular retrusion (decreased SNB angle) in two patients (patients 2 and 3).

Three-dimensional reconstructed images by MDCT also demonstrated the craniofacial manifestations shared by all four patients such as true/relative macrocephaly with maxillofacial hypoplasia, dolichocephaly, and mandibular anomalies characterized by thick and flat head of the condylar process, short condylar neck, narrow mandibular notch, and antegonial notching (Fig. 4). Calcified falx cerebri were also noted in all patients.

Table 2 Oral and dental features in four patients with Costello syndrome

	Patient				
	1	2	3	4	Total
Open mouth	+	+	+	+	4/4
Thick lips	+	+	+	+	4/4
Gingival hypertrophy	+	+	+	+	4/4
Gingivitis	−	−	−	+	1/4
Dental caries	−	−	−	+	1/4
Occlusal attrition	+	+	+	−	3/4
Relative macrocephaly with facial bone hypoplasia	+	+	+	+	4/4
High-arched palate	−	+	+	+	3/4
Convex face	+	+	+	−	3/4
Maxillary overhang	+	−	−	−	1/4
Mandibular retrusion	−	+	+	−	2/4
Malocclusion	O	−	C	O	3/4
Small dental arch	−	+	+	+	3/4
Maxilla	U	U	N	N	
Mandible	U	N	R	R	
Hypodontia	−	−	+	−	1/4
Conic teeth	−	−	−	+	1/4

+, present; −, absent; C, cross bite; O, open bite; N, narrow dental arch; R, rectangle dental arch; U, U-shaped dental arch.

DISCUSSION

We performed thorough evaluation of craniofacial and dental features in four patients with Costello syndrome. As previously

Table 3 Dental arch measurements in four patients

Patient	1		2		3		4	
	L1	L2	L1	L2	L1	L2	L1	L2
Maxilla	1.25	−0.67	−2.06	−2.90	−1.61	−2.52	−0.91	−1.04
Mandibular	0.79	−0.38	2.50	−0.06	−3.30	−1.98	−3.86	−2.42
	WC	WE	WC	WE	WC	WE	WC	WE
Maxilla	0.97	−0.02	−1.31	−2.88	−4.14	−2.80	−1.45	−1.52
Mandibular	0.97	0.51	−2.98	−1.49	−1.66	−0.24	−3.02	−2.53

WC and WE represent the distance between the primary cuspids (the cuspids), and the primary second molars, respectively. L1 represents the distance between the central point of the incisors and the line connecting the primary cuspids of both sides, and L2 represents the distance between the central point of the incisors and the line connecting the primary second molars of both sides. Unit, S.D.

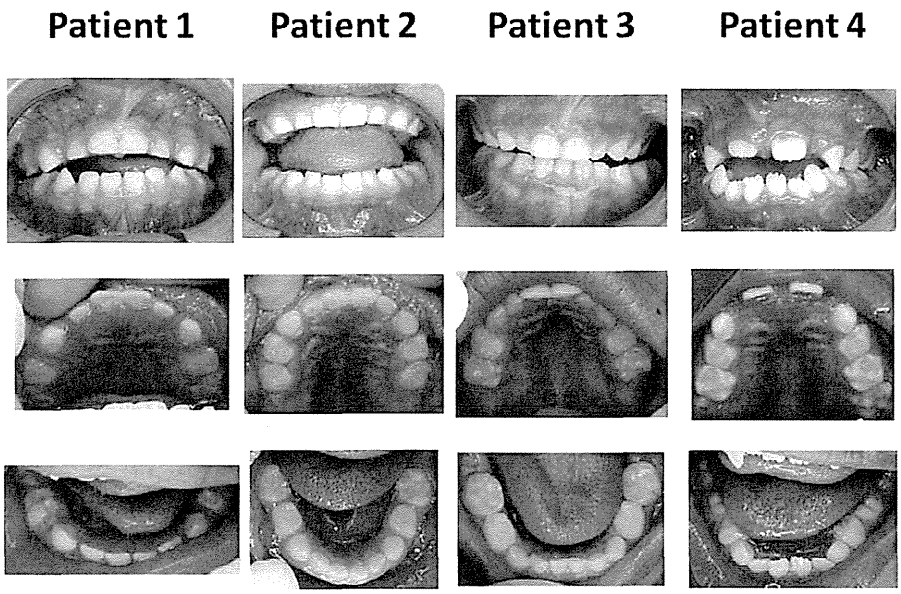

Fig. 1 Oral photographs of four patients. Patients 2, 3 and 4 showed occlusal attrition, high-arched palate and small dental arch. Patient 4 showed dental caries, gingivitis and conic teeth.

Fig. 2 Multi-detector row computed tomography (MDCT)-synthesized panoramic radiograph of Patient 3 at 6 years of age. Note the missing lower second premolar on left side (arrow).

reported, our patients showed true/relative macrocephaly and gingival hypertrophy (all patients). In addition, they exhibited malocclusion, occlusal attrition, small dental arches, microdontia, and convex face (three patients). Dental caries, conic tooth and gingivitis were noted in one patient, and hypodontia was noted in another patient. Enamel hypoplasia, an occasionally reported feature in patients with Costello syndrome, was not apparent in any of our patients.

True/relative macrocephaly is a well-known feature of patients with Costello syndrome. In this study, MDCT images showed macrocephalic skull in all four patients. In addition, facial bone hypoplasia was also evident which was associated with malformed mandible characterized by thick and flat head of the condylar process, short condylar neck, narrow mandibular notch, and antegonial notching on MDCT (Fig. 4). Antegonial notching is a feature seen in several congenital malformation syndromes associated with facial bone dysplasia, such as Treacher Collins syndrome, Nager syndrome and Pierre-Robin syndrome (Becker et al. 1976). Facial skeletal maldevelopment should be considered a feature of Costello syndrome.

Occlusal attrition is a finding that was frequently observed in our patients (patients 2, 3, 4). While the causes of attrition are diverse, malocclusion and habits such as bruxism and clenching are main possible causes. In view of behavioral characteristics of irritability of patients with Costello syndrome, habits such as teeth clenching might be a major cause for attrition.

It is of interest to know whether there are phenotypic similarities in craniofacial and dental features among Noonan-related disorders

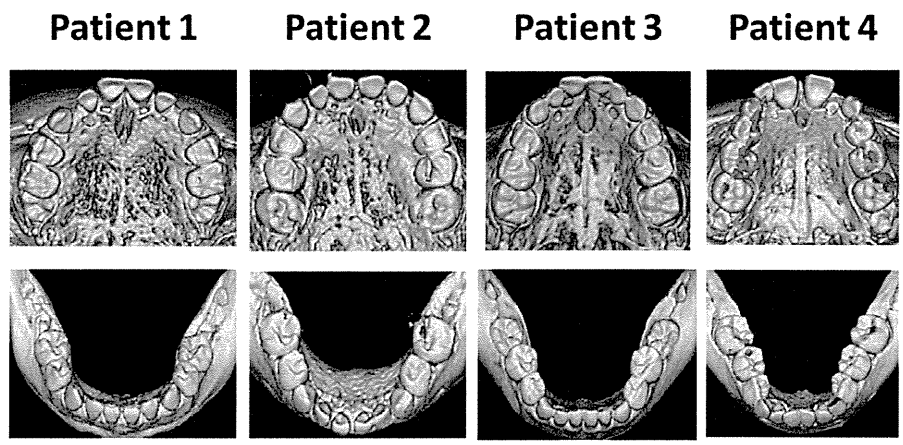

Fig. 3 Multi-detector row computed tomography (MDCT)-synthesized upper and lower dental arches in all four patients. Small dental arches are noted in three patients (patients 2, 3 and 4). Patient 2 exhibited a U-shaped dental arch in the maxilla and narrow dental arch in the mandible; Patients 3 and 4 exhibited narrow dental arches in the maxilla and rectangle arches in the mandible.

Table 4 Tooth size measurements in four patients

Patient	1		2		3		4	
	Right	Left	Right	Left	Right	Left	Right	Left
Maxillary								
Primary teeth								
Central incisor	0.54	0.54	−1.08	−0.54	−0.45	−0.45		
Lateral incisor	−2.00	−1.78	−1.56	−1.56	−2.44	−2.44	−0.49	
Cuspid	−1.22	−0.98	−1.22	−1.71	−0.73	−0.73	−0.98	−0.24
First molar	−2.39	−2.61	−2.17	−1.96	−1.09	−0.87	−0.43	−0.43
Second molar	−3.33	−3.16	−3.68	−3.51	−1.93	−1.58	−1.05	−0.53
Permanent teeth								
Central incisor							0.24	0.98
First molar							−1.95	−1.95
Mandibular								
Primary teeth								
Central incisor	0.31	0.00	−0.31	0.00	−1.00	−0.67		
Lateral incisor	1.21	1.52	0.00	−0.30	−0.83	−1.39		
Cuspid	0.31	0.31	−0.31	−0.63	−0.33	0.00	1.00	1.33
First molar	−1.30	−1.52	−1.30	−1.30	−0.60	−0.40	0.20	0.00
Second molar	1.04	1.04	−1.88	−1.46	0.00	−0.20	0.98	1.18
Permanent teeth								
Central incisor							−0.56	−0.83
Lateral incisor							−0.51	0.00
First molar							1.50	1.83

Tooth size represents the distance from the medial to the distal. Unit, S.D.

(RASopathies), including Noonan syndrome, CFC syndrome and Costello syndrome. However, a detailed investigation about craniofacial and dental findings has not yet been done. Recently, Goodwin et al. (2012) studied craniofacial and dental development in CFC syndrome based on 32 patients as the first large cohort study and found characteristic findings of the syndrome, including macrocephaly, convex facial profile, malocclusion with open bite, posterior cross bite, dental crowding, and high-arched palate. Among these features of CFC syndrome, macrocephaly, convex facial profile, malocclusion and high-arched palate were features noted in our patients with Costello syndrome as well. Unfortunately, as the evaluations of CFC syndrome by Goodwin et al. were mainly based on physical examination, more detailed evaluation regarding, such as dental arches, tooth size, and relationships between craniofacial, dental and skeletal structures have not been fully provided.

We used MDCT as a substitute for cephalometric, panoramic and dental cast studies. To our knowledge, this is the first study of thorough craniofacial and dental evaluation by using MDCT in Costello syndrome. As intellectual disability is common in Costello syndrome, these conventional cephalometric, panoramic and dental

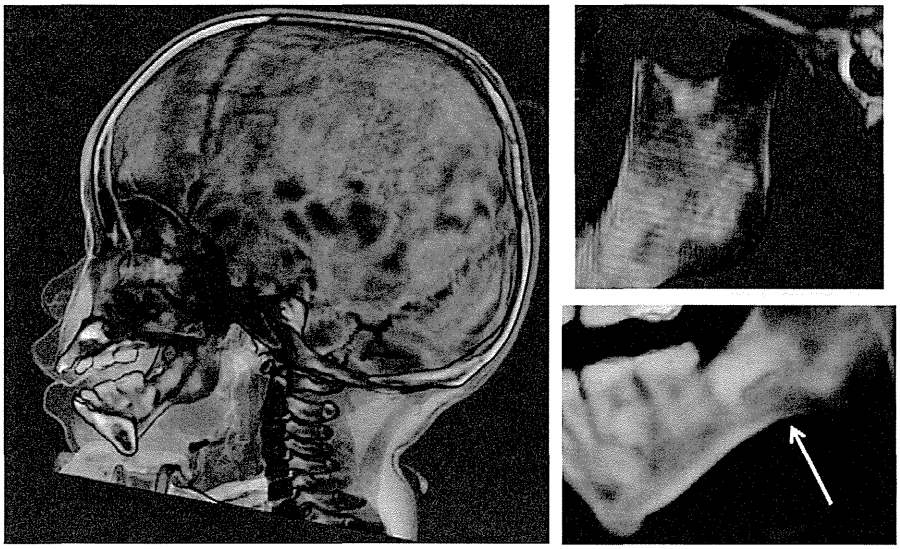

Fig. 4 Multi-detector row computed tomography (MDCT)-synthesized lateral radiograph (left) and close view of mandible (right) of Patient 3 at age of 6 years. Note the macrocephalic skull with hypoplastic facial bones (left). Mandibular anomalies are also noted, characterized by thick and flat head of the condylar process, short condylar neck, narrow mandibular notch (right upper) and antegonial notching (right lower).

Table 5 Lateral cephalometric analysis with MDCT of four patients

Patient	1	2	3	4
Skeletal				
Convexity	7.85	3.47	5.29	0.50
A-B plane	−0.12	−0.95	−1.78	0.76
SNA	4.06	−1.78	−1.78	−1.21
SNB	0.42	−2.89	−2.61	−1.14
Facial angle	−1.39	−1.54	1.39	0.53
SNP	−1.14	−2.99	−3.13	−1.56
Y axis	0.00	−0.15	−0.45	−0.84
SN-S·Gn	0.06	1.68	3.29	1.40
Mandibular plane	1.18	0.00	0.74	0.94
Gonial angle	0.77	−1.23	0.29	0.93
GZN	−0.12	2.33	2.51	2.09
FH to SN	−0.38	1.97	3.98	2.16
Dental				
U-1 to FH plane	2.37	−2.62	−0.31	4.44
U-1 to SN plane	3.12	−1.10	−2.41	3.02
L-1 to mandibular	1.17	4.94	−1.88	−1.28
Interincisal	−3.04	−2.04	0.80	−2.41
Occlusal plane	2.36	1.17	−0.69	−1.23

Unit, S.D.

cast studies are often difficult to perform, especially in the infantile period when patients tend to show marked irritability. MDCT is a useful tool for precise evaluation of craniofacial and oral manifestations in multiple congenital anomaly/intellectual disability syndromes (Hirai et al. 2011).

In conclusion, characteristic craniofacial and oral features frequently noted in patients with Costello syndrome might be true/relative macrocephaly with facial bone hypoplasia, gingival hypertrophy, malocclusion, occlusal attrition, small dental arches, microdontia, and convex face. Craniofacial and dental abnormalities are common in Costello syndrome patients and comprehensive dental care should be provided from early infancy.

ACKNOWLEDGMENTS

The authors are grateful to Professor Takahide Maeda for his helpful advice. We also thank Dr Kensuke Matsune, Dr Kenji Shimizu, Dr Yasuo Takahashi, and Hitoshi Yabe for their invaluable assistance. This study was funded in part by a Grant for the Support of Projects for Strategic Research at Private Universities by the Ministry of Education, Culture, Sports, Science and Technology (MEXT; 2008–2012), and by a grant from the Ministry of Health, Labour and Welfare, Japan.

REFERENCES

Abe Y, Aoki Y, Kuriyama S et al. 2012. Prevalence and clinical features of Costello syndrome and cardio-facio-cutaneous syndrome in Japan: findings from a nationwide epidemiological survey. Am J Med Genet A 158A:1083–1094.

Aoki Y, Niihori T, Kawame H et al. 2005. Germline mutations in HRAS proto-oncogene cause Costello syndrome. Nat Genet 37:1038–1040.

Becker MH, Coccaro PJ, Converse JM. 1976. Antegonial notching of the mandible: an often overlooked mandibular deformity in congenital and acquired disorders. Radiology 121:149–151.

Delrue MA, Chateil JF, Arveiler B, Lacombe D. 2003. Costello syndrome and neurological abnormalities. Am J Med Genet A 123A:301–305.

Der Kaloustian VM, Moroz B, McIntosh N, Watters AK, Blaichman S. 1991. Costello syndrome. Am J Med Genet 41:69–73.

Di Rocco M, Gatti R, Gandullia P, Barabino A, Picco P, Borrone C. 1993. Report on two patients with Costello syndrome and sialuria. Am J Med Genet 47:1135–1140.

van Eeghen AM, van Gelderen I, Hennekam RC. 1999. Costello syndrome: report and review. Am J Med Genet 82:187–193.

Fukawa A. 2008. Orthodontic consideration of quadruplets, compared to themselves and their parent at dento-maxilla-faical form. J Jpn Assoc Orthod 19:21–29.

Goodwin AF, Oberoi S, Landan M et al. 2012. Craniofacial and dental development in cardio-facio-cutaneous syndrome: the importance of ras signaling homeostasis. Clin Genet Sep 4. doi: 10.1111/cge.12005. [Epub ahead of print].

Hennekam RC. 2003. Costello syndrome: an overview. Am J Med Genet C Semin Med Genet 117C:42–48.

Hirai N, Yamauchi T, Matsune K et al. 2010. A comparison between two dimensional and three dimensional cephalometry on lateral radiographs and multi detector row computed tomography scans of human skulls. Int J Oral Med Sci 9:101–107.

Hirai N, Matsune K, Ohashi H. 2011. Craniofacial and oral features of Sotos syndrome: differences in patients with submicroscopic deletion and mutation of NSD1 gene. Am J Med Genet A 155A:2933–2939.

Iizuka T, Ishikawa F. 1957. Normal standards for various cephalometric analysis in Japanese adults. Nippon Kyosei Shika Gakkai Zasshi 16:4–12.

Johnson JP, Golabi M, Norton ME et al. 1998. Costello syndrome: phenotype, natural history, differential diagnosis, and possible cause. J Pediatr 133:441–448.

Kato K. 1979. [Studies on growth and development of dentition in Japanese children – examination of the longitudinal casts from deciduous dentition of 3-year-old to permanent dentition (author's transl)]. Shika Gakuho 79:991–1027. (In Japanese.)

Kawame H, Matsui M, Kurosawa K et al. 2003. Further delineation of the behavioral and neurologic features in Costello syndrome. Am J Med Genet A 118A:8–14.

Otsubo J. 1964. A longitudinal study of dental development between 6–13 years of age: growth changes of dentition. Nippon Kyosei Shika Gakkai Zasshi 23:182–190.

Rauen KA, Schoyer L, McCormick F et al. 2010. Proceedings from the 2009 genetic syndromes of the Ras/MAPK pathway: from bedside to bench and back. Am J Med Genet A 152A:4–24.

Teebi AS, Shaabani IS. 1993. Further delineation of Costello syndrome. Am J Med Genet 47:166–168.

Yamauchi T, Hirai N, Matsune K et al. 2010. Accuracy of tooth development stage, tooth size and dental arch width in multi detector row computed tomography scans of human skulls. Int J Oral Med Sci 9:108–114.

Zampino G, Mastroiacovo P, Ricci R et al. 1993. Costello syndrome: further clinical delineation, natural history, genetic definition, and nosology. Am J Med Genet 47:176–183.

Congenital Anomalies
THE JAPANESE TERATOLOGY SOCIETY
doi:10.1111/j.1741-4520.2012.00362.x
Congenital Anomalies 2013; **53**, 49–53

CASE REPORT

Patient with terminal 9 Mb deletion of chromosome 9p: Refining the critical region for 9p monosomy syndrome with trigonocephaly

Norimasa Mitsui[1], Kenji Shimizu[2], Hiroshi Nishimoto[3], Hiroshi Mochizuki[4], Masao Iida[1], and Hirofumi Ohashi[2]
[1]Department of Clinical Laboratory, Divisions of [2]Medical Genetics, [3]Neurosurgery, and [4]Metabolism and Endocrinology, Saitama Children's Medical Center, Saitama, Japan

ABSTRACT **We describe a patient with typical manifestations of 9p monosomy syndrome, including trigonocephaly and sex reversal. Array comparative genomic hybridization (CGH) revealed a 9p terminal deletion of approximately 9 Mb with the breakpoint at 9p23. We compared the deleted segments of 9p associated with reported cases of 9p monosomy syndrome with trigonocephaly. We did not identify a region that was shared by all patients; however, when only pure terminal or interstitial deletions that did not involve material from any other chromosome were compared, we identified a segment from D9S912 to RP11-439I6 of approximately 1 Mb that was deleted in every patient. We propose that this 1-Mb segment might be the critical region for 9p monosomy syndrome with trigonocephaly.**

Key Words: 9p monosomy, craniosynostosis, critical region, sex reversal, trigonocephaly

INTRODUCTION

Monosomy 9p syndrome [MIM 158170] is a rare but well-known chromosomal deletion syndrome characterized by distinct craniofacial features (including trigonocephaly), various systemic anomalies, developmental retardation, and occasional sex reversal in XY patients (Huret et al. 1988). Since Alfi et al. (1973) first described a patient with the syndrome, more than 100 patients, most with terminal deletions with breakpoints around 9p21-p23 based on chromosome G-band analysis, have been reported. Recent advances in molecular/cytogenetic techniques allow attempts to map the loci responsible for cardinal features of the syndrome, especially trigonocephaly and sex reversal. While *DMRT* genes, which map to the most terminal 9p24.3 band, have been elucidated as the genes responsible for sex reversal (Raymond et al. 1998; Ogata et al. 2001; Barbaro et al. 2009), no gene has yet been identified as definitively responsible for trigonocephaly. Moreover, previous studies have been inconsistent with regard to identification of the 9p regions that are responsible for trigonocephaly (Wagstaff and Hemann 1995; Christ et al. 1999; Kawara et al. 2006; Faas et al. 2007; Hauge et al. 2008; Swinkels et al. 2008; Shimojima and Yamamoto 2009). Here, we describe a patient with a terminal 9p deletion of approximately 9 Mb who has the typical clinical manifestations of 9p monosomy syndrome, including trigonocephaly and sex reversal.

Correspondence: Hirofumi Ohashi, MD, PhD, Division of Medical Genetics, Saitama Children's Medical Center, 2100 Magome, Iwatsuki-ku, Saitama-shi, Saitama 339-8551, Japan. Email: ohashi.hirofumi@pref.saitama.lg.jp

Received January 20, 2012; revised and accepted February 9, 2012.

CLINICAL REPORT

The girl patient was born by cesarean section after 38-week gestation to a 30-year-old gravida 2, para 1 mother and a 31-year-old father, both Japanese, healthy, and unrelated. The patient's birth weight was 2864 g (−0.5 SD), length 49.5 cm (+0.2 SD), and occipitofrontal head circumference 35.5 cm (+1.5 SD). The patient had a healthy older sister. The patient was referred to us at the age of 11 months because of developmental delay and skull deformity. The notable craniofacial features were trigonocephaly, ptosis of the eyelids, epicanthus, upslanting palpebral fissures, flat nasal bridge, broad nasal root, long philtrum, thin upper lip, and low-set ears. A skull computed tomography scan with 3D reconstruction confirmed trigonocephaly with metopic suture synostosis (Fig. 1). Fronto-orbital advancement with cranial reshaping was performed when she was 1 year and 3 months old. She showed normal female external genitalia. When the patient was 2 years old, an abdominal ultrasonography revealed a uterus, but no ovary or testis was detected. A test of human chorionic gonadotropin load suggested the existence of testis, while luteinizing hormone-releasing hormone load test revealed primary hypogonadism. She weighed 14 kg (−1.7 SD) and was 100.2 cm tall (−1.9 SD) at 5 years of age. Her development was moderately delayed, and her IQ was estimated to be around 40 with the Tanaka–Binet Intelligence Scale at the age of 6 years.

G-banding analysis at a resolution of 550-bands on metaphase chromosomes obtained from phytohemagglutinin-stimulated lymphocyte cultures from the patient revealed a distal deletion of the short arm of chromosome 9 with a breakpoint at 9p23 and an XY sex chromosome constitution (sex reversal) (Fig. 2). Her parents were chromosomally normal. Fluorescence *in situ* hybridization (FISH) using whole-chromosome painting probes for chromosome 9 and a subtelomeric probe for the short arm of chromosome 9 (both from Vysis/Abbott Molecular Inc., Des Plaines, IL, USA) revealed that the abnormal chromosome 9 did not contain translocated material from another chromosome. To further define the extent of the deleted region in 9p, we performed an array comparative genomic hybridization (CGH) analysis using the Agilent Human Genome 244 K CGH kit (Agilent Technologies, Santa Clara, CA, USA). The result showed a hemizygous 9.17 Mb terminal deletion of chromosome 9p and no other apparent pathogenic copy number variation was identified in the whole genome (Fig. 3). Her karyotype was designated as 46,XY,del(9)(p23).arr 9p23 (194 193-9 169 072)x1 dn. FISH analyses with bacterial artificial chromosome (BAC) clones spanning the region from 9p23 to 9p24 refined the breakpoint between the clones RP11-1134E16 (D9S2000) and RP11-74 L16 (D9S912) (Table 1). BACs containing *DMRT1* and *DMRT2*, both candidate genes for sex reversal (9p24.3), were confirmed to be in the deleted segment of 9p in the patient.